Available online at www.sciencedirect.com

ScienceDirect

Procedia CIRP 111 (2022) 308–312

www.elsevier.com/locate/procedia

12th CIRP Conference on Photonic Technologies [LANE 2022], 4-8 September 2022, Fürth, Germany

Dynamic control for LMD processes using sensor fusion and edge computing

Beñat Arejita[a,b,*], Iker Garmendia[c], Juan Fernando Isaza[a], Aitzol Zuloaga[b]

[a]*EXOM Engineering, Avenida Altos Hornos de Vizcaya 33, Barakaldo 48901, Spain*
[b]*UPV/EHU, Ingeniero Torres Quevedo Plaza 1, Bilbao 48013, Spain*
[c]*TEKNIKER, C. Iñaki Goenaga 5, Eibar 20600, Spain*

* Corresponding author. Tel.: +34-623-108-883; *E-mail address:* benat.arejita@exomengineering.com

Abstract

The quality of an LMD manufactured object highly depends on different process parameters such as the speed of powder deposition, the applied laser power, the powder feed rate, and other physical parameters such as the substrate temperature, resulting in a complex process. Consequently, applying corrections to the process parameters can be critical to improving the properties of the manufactured part. Some control approaches rely on open-loop techniques that use physical models and expert knowledge to adjust the tool path program in advance to compensate for deviations from the theoretical 3D model. Other approaches apply closed-loop control techniques to either control the melt pool during the process or adjust the tool path between layer depositions. This work presents a closed-loop control algorithm that dynamically controls three critical process parameters: the melt pool size, deposition speed, and standoff distance, combining data from a laser line profiler and a high-speed infrared camera.

Peer-review under responsibility of the international review committee of the12th CIRP Conference on Photonic Technologies [LANE 2022]

Keywords: Additive Manufacturing; Laser Metal Deposition; Dynamic Process Control; Edge Computing; Industry 4.0

1. Introduction

The laser metal deposition (LMD) technique produces components using a high-power laser that melts a metallic powder or wire, manufacturing the part in a layer-by-layer manner. This Additive Manufacturing (AM) method can produce or modify parts and molds by moving the laser beam and the material feeder following a tool path derived from a CAD drawing. To get an effective LMD system, it is essential to precisely control different process parameters such as the powder feed rate, the laser power, the beam width, the overlap percentage, the layer thickness, the energy density, or the cooling rate [1]. While the 3D components are being processed, the tool path geometry plays a critical part in the thermal effects that the material experiences. Thus, a poorly planned tool path can lead to overheating effects resulting in defects such as pores that can potentially change the mechanical characteristics of the component. The deposition direction also affects the overall temperature, where a direction from edge to center shows lower maximum temperatures compared to directions from the center to the edge. A zig-zag pattern from edge to center is a typical tool path strategy that minimizes both the maximum temperature of the part and the temperature difference in the edge area [2]. To obtain a uniform layer geometry, a continuous energy deposition control must be done as the geometry of a bead is closely related to the thermal conditions of the process. These geometry variations change the degree of overlap between adjacent beads resulting in a non-uniform layer height that differs from the target height of the layer. Consequently, it is essential to measure the actual height of the part to correct the experienced deviations during the process. Different research works have focused on different height measuring techniques. For instance, Tyralla et al. presented a work applying a dual laser triangulation system with a temperature

2212-8271
Peer-review under responsibility of the international review committee of the12th CIRP Conference on Photonic Technologies [LANE 2022]
10.1016/j.procir.2022.08.026

field camera to measure the melt pool geometry and the amount of bead overlapping that results in height deviations [3]. The use of structured light has also been explored to measure layer deviations between layer depositions, Garmendia et al. [4]. Other methods rely on a coaxial measurement of the deposition height by using different techniques such as Optical Coherence Tomography (OCT) or the combination of optical setups and CCD cameras as presented by Donadello et al. [5]. Thus, when a high degree of automation is needed, a closed-loop sensor-based approach can be used by measuring the layer height and adapting the toolpath to compensate for the errors. This approach makes it possible to obtain a high degree of independence concerning process parameters and materials used [6]. The control of the LMD process can be done following different approaches. Some research work has focused on model-based open-loop control methods by modifying the theoretical path in a post-processing phase that changes the path with the information obtained from the models [7]. Nevertheless, a closed-loop approach is more suitable for adaptive control techniques by measuring the melt pool to adapt the applied laser power dynamically or by measuring the layer height to adapt the deposition height or speed [8-10].

Effective control of component geometry and material morphology remains major challenges in LMD [11]. Layer by layer manufacturing technologies are in general highly complex processes involving several localized heating and cooling steps. Therefore, in-line monitoring and real-time control solutions are needed for a successful quality assurance in LMD. A few studies measure geometry fidelity either offline [12, 13], or online [14, 15, 16] using stereo cameras, height triangulation sensor and line scanners. Tang et al [17] and Arrizubieta et al [18] determined the temperature during the process as well as the weld height of each individual layer after deposition, using a triangulation sensor and pyrometer. Among others, authors found that component slopes or welding seam-ends can cause faulty measurements due to the tilted surface and the small measuring area of the pyrometer.

Nomenclature

Q_i	normalized unit quaternions (rotation quaternions)
R	orthogonal matrix for the rotation by the unit quaternion provided by the robot
WO_{TCP}	tool center point to working object coordinate transformation matrix
$TCP_{ESC.}$	Scanned point to tool center point coordinate transformation matrix
P	scanned point
P_{WO}	scanned point in working object coordinate system
%v	velocity percentage change
$\%v_{max.}$	maximum velocity percentage change
Δz	layer height deviation
z_{target}	ideal layer height from CAD model
$z_{measured}$	measured layer height after deposition
Δz_{max}	maximum layer height deviation

The current work presents a setup for an in-process LMD layer height correction using an embedded process controller that adapts the melt pool size, the material deposition speed, and the standoff distance (SOD), using data from a laser line profiler and a high-speed IR camera.

2. Experimental set-up

The control of the LMD process is done by dynamically controlling three main parameters in real-time; the standoff distance, the deposition speed, and the melt-pool size. To achieve this, the experimental setup used in the implementation of this work integrates two main interconnected components: an ABB4400 industrial robot and the embedded LMD process controller. The LMD controller can be installed directly in the LMD laser head due to its small form factor. The controller is based on a ZCU3EG Zynq Ultrascale+ SoC from Xilinx that combines an FPGA for real-time highly parallel processing tasks, a quad-core ARM cortex-A53 processor, and a dual-corARM cortex-R5F. The robot runs the tool path controller and constantly sends the tool center point (TCP) and the rotation quaternions to the LMD controller. The LMD controller is connected to an NIT Tachyon 1024 micro-core MWIR camera and a Gocator 2440-2B laser line profiler. Fig. 1 shows the experimental setup with the industrial robot and the end of the arm tooling components.

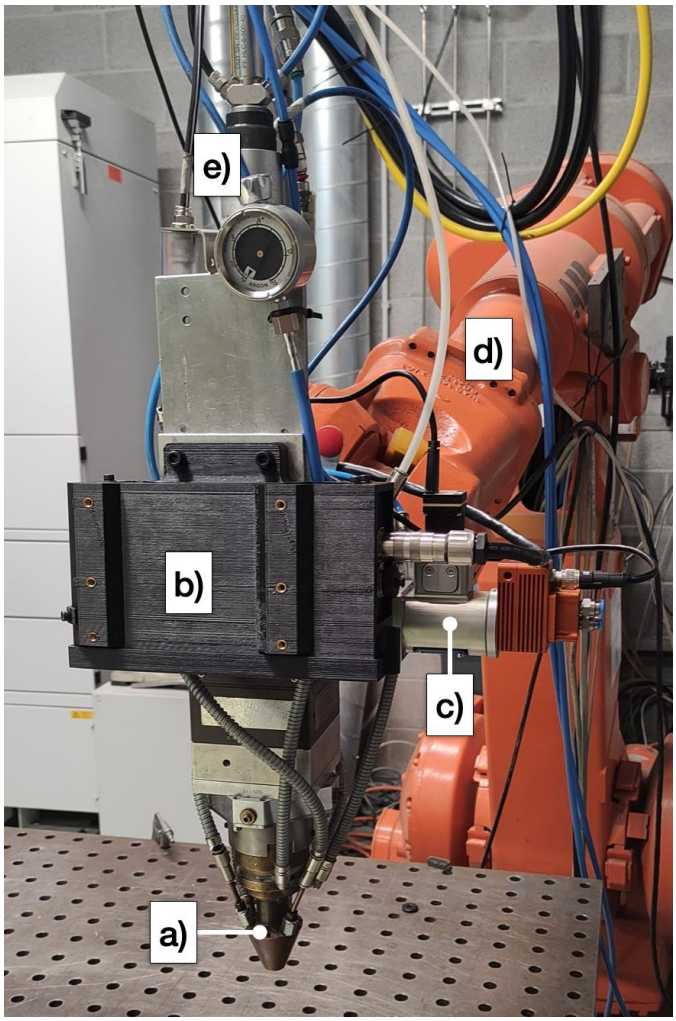

Fig. 1. Experimental setup. Industrial robot and end of the arm tooling components: a) powder nozzle mounted on a precitec optical head, b) Gocator laser line scanner, c) coaxial camera module with a coupled MWIR camera, d) 6-AXIS ABB robot and e) laser fiber input.

Thus, the LMD controller gathers the data from three different sources; the TCP position from the robot, the melt-pool temperature information from the IR camera, and the layer profile points from the line profiler. These data are then processed in real-time to generate the correction values that are applied by the robot.

After every computation iteration, the control card sends back the correction parameters to be applied to the robot. Thus, the control loop is closed, and the height deviation correction, deposition speed, and laser power are updated for every control cycle. The processing of each layer is done in two steps. In the first step, the existing layer surface is measured, and the deviations are stored. In the second step, the stored deviation map is used to do the actual correction during the deposition.

3. Surface height measurement and coordinate transformation

In order to measure the height deviations of each layer from the CAD model, a measurement pass is done by the robot to scan the recently deposited layer with the line profiler, generating a point cloud of the layer as a result. As the point cloud is measured with the reference system of the laser line profiler, the coordinate transformation defined in eq. 1 must be done to convert each point of the point cloud to the work object reference system.

$$\boldsymbol{P_{WO} = WO_{TCP} \cdot TCP_{ESC} \cdot P'} \qquad (1)$$

Each point **P** is converted into the TCP coordinate system using its transpose form **P′** and the **TCP**$_{ESC}$ transformation matrix, calculated in the system calibration phase, and remains unchanged as the relation between the profiler and the TCP is fixed, considering that the laser line scanner is rigidly mounted at the end of the arm of the robot. The converted points are then transformed into the work object reference system using the transformation matrix **WO**$_{TCP}$, which must be continuously recalculated with the state information sent by the robot.

$$\boldsymbol{WO_{TCP}} = \begin{bmatrix} RI_{00} & RI_{01} & RI_{02} & TCP_X \\ RI_{10} & RI_{11} & RI_0 & TCP_Y \\ RI_0 & RI_0 & RI_0 & TCP_Z \\ 0 & 0 & 0 & 1 \end{bmatrix}$$

Where RI_{xy} are the elements of the inverse orthogonal transformation matrix **R** and TCP_X, TCP_Y and TCP_Z are the instantaneous coordinatizes of the TCP that are continuously updated as the process is being executed.

$$\boldsymbol{R} = \begin{bmatrix} (Q_1{}^2 - Q_2{}^2 - Q_3{}^2 + Q_4{}^2) & 2(Q_1Q_2 + Q_3Q_4) & 2(Q_1Q_3 - Q_2Q_4) \\ 2(Q_1Q_2 - Q_3Q_4) & (Q_2{}^2 - Q_1{}^2 - Q_3{}^2 + Q_4{}^2) & 2(Q_2Q_3 + Q_1Q_4) \\ 2(Q_1Q_3 + Q_2Q_4) & 2(Q_2Q_3 - Q_1Q_4) & (Q_3{}^2 - Q_1{}^2 - Q_2{}^2 + Q_4{}^2) \end{bmatrix}$$

The **WO**$_{TCP}$ matrix must be computed every time a new state update comes from the robot. This processing is done on the fly by the embedded LMD controller using its real-time processing capabilities, as the FPGA of the ZCU3EG system on chip takes advantage of the high throughput low latency parallel processing capabilities it offers.

4. Control strategy

As a first step, the deposition path is calculated from a CAD model using a trajectory generator, and the trajectories are then sent to the six-axis robot. In order to measure the height deviations during the process, each layer deposition is divided into two phases as mentioned previously: the surface measurement phase and the deposition phase.

Firstly, the robot executes a measurement path, and the previously deposited layer is scanned using the laser line profiler, generating a layer height deviation map. In the deposition phase, the robot starts executing the actual tool path to manufacture the part and keeps sending the TCP information to the control card. The control card then uses the TCP coordinates to determine the height error in the deviations map computed in the measurement phase. The height deviation is used to compute the percentage variation of the deposition speed, as it can be seen in Eq. 2 (Garmendia et al. [10]). If the measured height is lower than the target, the deposition speed will slow down to deposit more material. In contrast, if the measured height is higher than the target, the deposition speed will increase to deposit less material in that area.

$$\%v = 50 + \left(\frac{\%v_{max}}{2} \cdot \frac{\Delta z}{|\Delta z_{max}|}\right) \qquad (2)$$

$$\Delta z = z_{target} - z_{mearued}$$

To illustrate this, Fig. 2 shows an example of the deposition speed percentage modification, the parameters $\%v_{max}$ and Δz are set to 20 and 1, respectively; allowing a change in velocity of +/-10% where the maximum considered height deviation is +/-1 mm (the measured deviation is saturated to the max deviation). As the robot cannot execute velocity changes greater than 100%, the nominal velocity value is always double the desired value, and the velocity percentage change is thus centered at 50%.

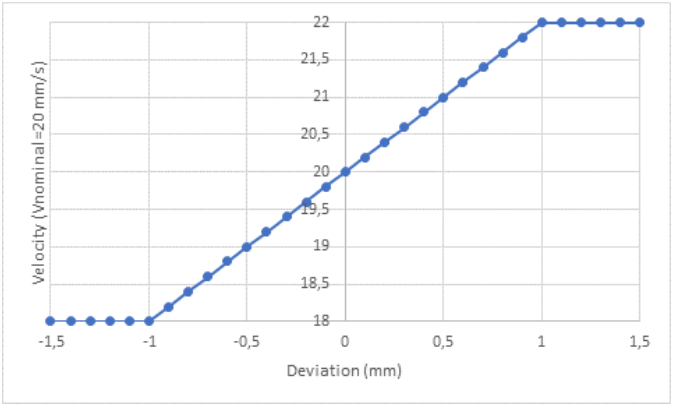

Fig. 2. Example of the deposition velocity percentage modification curve as a function of measured height deviation. $\%v_{max} = 20\%$, $\Delta z = 1$ mm and resulting nominal deposition velocity of 20 mm/s

In parallel, the stability of the melt pool is controlled in real-time by applying the method described by Panadeiro et al. [19] and using the IR camera that can acquire images at speeds up to 1000 frames per second.

Concerning the IR camera, it is essential to consider the pixel-to-pixel differences (Non-Uniformity or fixed-pattern noise) for a given input flux or input radiance due to the temperature of the material, thus limiting errors in the measurements of the molten pool and further improving the quality of the manufactured parts. For this reason and prior to the experimental tests, a calibration procedure against a black body radiator, as described in previous research work [20], was conducted to compensate for the Non-Uniformity effects and obtain better radiometric calculations.

5. Results and discussion

The experiment was conducted using a 2000 W fiber laser (IPG, YLS-2000-CT), and the laser beam was guided to the working area by a 0.6 mm diameter circular fiber and an optical head by Precitec. A 6-axis ABB 4400 robot provided the movement of the laser head for the measurement and deposition phases. The material was deposited on a 15 mm thick C45E carbon steel substrate, where a Sulzer Metco Twin-10C powder feeder delivered Metcoclad 316L-Si stainless steel powder (Oerlikon Metco). The generated deposition tool paths consisted of an outer perimeter and a zig-zag filling strategy with the filling angle alternating between +45º and -45º with respect to the sides of the cube, as shown in Fig. 3.

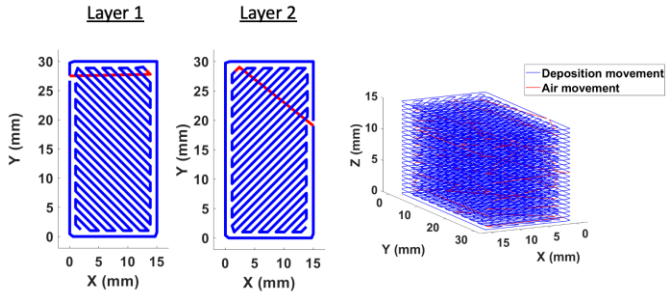

Fig. 3. Deposition toolpath strategy with an alternating 45ª zig-zag filling pattern withing rectangle outer perimeter.

To test the performance of the control strategy, the material was deposited on a substrate that was previously machined. The precision of the scanner in depth was 50 μm, and the vertical position of the robot was corrected constantly to adapt it to the growth of the part. For this reason, the error with which the height was being updated corresponded to the measurement error of the scanner together with the trajectory error that the robot. The machining generated a step with a height difference of 2 mm between the top and the bottom sides. The test aimed to validate the adaptation of the vertical position of the robot during the depositing process to the height differences. On the other hand, the variation of the robot movement speed leads to a variation of the material feed rate, so it was dynamically adjusted based on the scanned height to reduce the difference between the upper and lower part of the generated step, and therefore recover a plane deposition. The main process parameters are listed in Table 1.

The configuration of the deposition velocity percentage modification was {%v}_{max}=10 and Δzmax=1. This configuration constrained the controller to apply maximum height corrections of 1 mm and a +/- 10% velocity change.

Table 1. Main process parameters.

Process parameter	Value	Units
Laser power	1500	Watt
Robot velocity	15	mm/s
Powder feed rate	10	g/min
Distance between beads	1	mm
Layer height	0.7	mm

When the process started, the measurement phase detected a height deviation of 2 mm in the machined part of the deposition surface. This led to applying an offset to the theoretical tool path standoff distance of 1 mm and a variation in the velocity of 45 % from the nominal value (13.5 mm/s). For the area where the substrate was not machined, the standoff distance offset remained around 0 mm, and the deposition velocity remained in the nominal value (15 mm/s).

This effect is clearly seen in Fig. 4 and Fig.5. As the workpiece grows, it can be seen how the extra material deposition that occurs in the machined area due to the decrease in deposition velocity starts to even out the surface height through the piece.

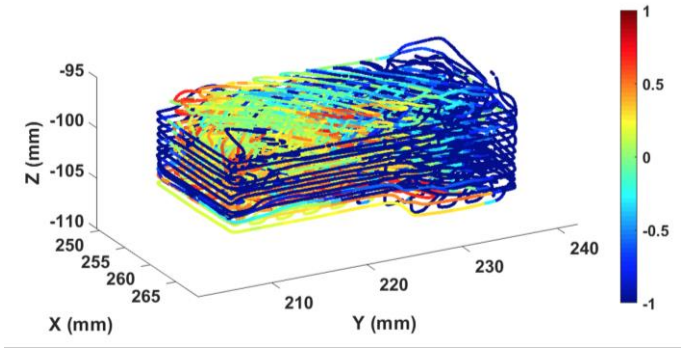

Fig. 4. Commanded position and height correction in mm.

By the fourteenth layer, the control strategy was able to compensate for the initial 2 mm deviation of the machined part. The blue-colored paths and points in Fig. 4 and Fig. 5 depict the measured height deviation and the corresponding decrease in velocity, whereas the yellow paths and points depict that the tool path was not modified. In contrast, the red-colored lines and points depict the extra growth that happens due to the complex deposition and melt pool dynamics, and it can be seen that the controller compensates for those effects by increasing the deposition velocity.

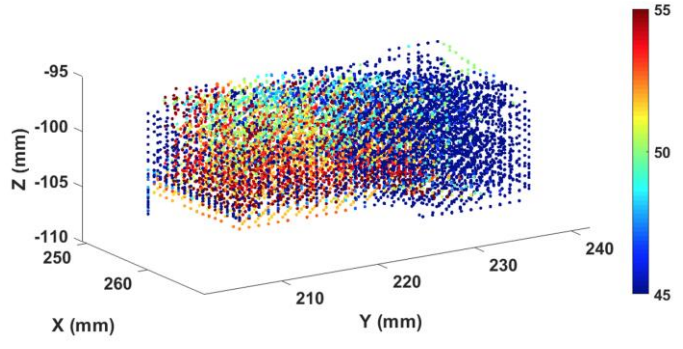

Fig. 5. Commanded position and velocity percentage correction.

The tests were run with and without dynamic height control to compare the results of the strategies. Fig.6 shows how the errors were compensated with the control strategy. However, the measurement phase introduced an average increase of 17% to the layer deposition time.

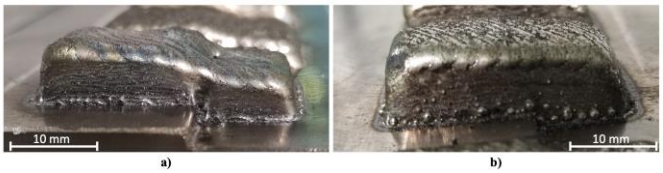

Fig. 6. Results of test specimen. a) Without dynamic control, b) with dynamic height and velocity percentage control.

4. Conclusion

A laser line profiler and a high-speed IR camera were used to control an LMD process in a robotic cell. The control strategy consisted of the dynamic correction of the standoff distance (nozzle-to-part distance), the deposition velocity (feed rate), and melt pool temperature (laser power) using an embedded controller to do the real-time computation. Each layer deposition was divided into two different phases. While in the measurement phase, mainly between the last point on the surface N-1 and the first point of the surface N, the layer was scanned to generate the deviation map. The deposition phase uses the previously computed deviations to make dynamic adjustments to the deposition path on the fly, reducing higher temperature fluctuations and extreme microstructural changes between the layers that can result from stopping the process to analyze the data and generate new paths. Also, during the deposition phase, the temperature of the bead is being measured to control the laser power, resulting in a more homogeneous temperature distribution in the layer and reducing thermally induced stresses during manufacturing. Different tests were carried out with and without the presented control strategy on a previously machined surface to evaluate the performance. The results showed that the controller could compensate for the height deviations at the cost of an average 17 % increase in the layer processing time and move forward to first-time-right manufacturing.

Acknowledgements

The work presented in this publication has received funding from the European Union's Horizon 2020 research and innovation programme within the framework of the Pulsate Project funded under grant agreement No [951998] as part of the experiment CESFAM selected in the Pulsate 1st TTE open call. PULSATE is supported by the Photonics Public Private Partnership.

References

[1] Ghosal P, Majumder MC, Chattopadhyay A. Study on direct laser metal deposition. Materials Today Procedings 5, 2018, p. 12509-12518.
[2] Petrat T, Winterkorn R, Graf B, Gumenyuk A, Rethmeier M. Build-up strategies for temperature control using laser metal deposition for additive manufacturing. Weld World 2018, 62, p. 1073-1081.
[3] Tyralla D, Köhler H, Seefeld T, Thomy C, Narita R. A multi-parameter control of track geometry and melt pool size for laser metal deposition. Procedia CIRP 94, 2020, p. 43.
[4] Garmendia I, Leunda J, Pujana J, Lamikiz A. In-process height control during laser metal deposition based on structured light 3D scanning. Procedia CIRP 68, 2018, p. 375-380.
[5] Donadello S, Motta M, Demir AG, Previtali B. Coaxial laser triangulation for height monitoring in laser metal deposition. Procedia CIRP 74, 2018, p. 144-148.
[6] Buhr M, Weber J, Wenzl JP, Möller M, Emmelmann C. Influences of process conditions on stability of sensor controlled robot-based laser metal deposition. Procedia CIRP 74, 2018, p. 149-153.
[7] Chen L, Yu T, Chen Y, Wang W. Slicing strategy and process of laser direct metal deposition (DMD) of the inclined thin-walled part under open-loop control. Rapid Prototyping Journal, 2022, 28-1, p. 68-86.
[8] Liu Y, Wang L, Brandt M. Model predictive control of laser metal deposition. Int J Adv Manuf Technol, 2019,105, p. 1055-1067.
[9] Song L, Bagavath-Singh V, Dutta B, Mazumder J. Control of melt pool temperature and deposition height during direct metal deposition process. Int J Adv Manuf Technol, 2012, 58, p. 247-256.
[10] Garmendia I, Pujana J, Lamikiz A, Flores J, Madarieta M. Development of an Intra-Layer Adaptive Toolpath Generation Control Procedure in the Laser Metal Wire Deposition Process. Materials 2019, 12:352.
[11] Rodriguez J P, Peña C, Rodriguez E. Atlas_GcodeSender: a Graphical User Interface for Control of a Robotics Additive Manufacturing Platform. 2018 IEEE International Conference on Mechatronics and Automation (ICMA), 2018, pp. 671-676.
[12] Heralić A, Christiansson AK, Lennartson B. Height control of laser metal-wire deposition based on iterative learning control and 3d scanning. Optics and lasers in engineering, 2012, 50 (9), pp. 1230-1241.
[13] Li Z, Liu X, Wen S, He P, Zhong K, Wei Q, Shi Y, Liu S. In situ 3d monitoring of geometric signatures in the powder-bed-fusion additive manufacturing process via vision sensing methods. Sensors (basel, switzerland), 2018, 18 (4).
[14] Faes M, Vogeler F, Coppens K, Valkenaers H, Abbeloos W, Goedemé T, Ferraris E. Process Monitoring of Extrusion Based 3D Printing via Laser Scanning. International Conference on Polymers and Moulds Innovations (PMI2014), 2014, 6.
[15] Binega E, Yang L, Sohn H, Cheng J C P. Online Geometry Monitoring during Directed Energy Deposition Additive Manufacturing Using Laser Line Scanning. Precision Engineering, 2022, 73, pp. 104–114.
[16] Liu R, Wang Z, Sparks T, Liou F, Nedic C. Stereo Vision-Based Repair of Metallic Components. Rapid Prototyping Journal 2017, 23 (1), pp. 65-73.
[17] Tang L, Landers R G. Layer-to-Layer Height Control for Laser Metal Deposition Process. ASME. J. Manuf. Sci. Eng. 2011, 133 (2).
[18] Arrizubieta J I, Ruiz J E, Martinez S, Ukar E, Lamikiz A. Intelligent Nozzle Design for the Laser Metal Deposition Process in the Industry 4.0. Procedia Manufacturing, 2017, 13, pp. 1237-1244.
[19] Panadeiro-Castro V, Rodriguez-Araujo J, Garcia-Diaz A, Vergara G. Medium wavelength infrared (MWIR) imaging for high speed control of laser metal deposition (LMD). Lasers in Engineering 2018, 39, pp. 67-75.
[20] Arejita B, Isaza J F, Roldán C, Zuloaga A. Applying Edge Artificial Intelligence to Closed Loop Real Time Control and Monitoring of Laser Based Battery Pack Welding. Procedings of the 41st annual International Congress on Applications of Lasers & Electro-Optics ICALEO, 2021.